Plasters with mixed-in crystallization inhibitors: Results of a 4-year monitoring of on-site application

Lubelli, B.; des Bouvrie, Ernst ; Nijland, Timo G.; Kamat, A.A.

DOI
10.1016/j.culher.2022.10.016

Publication date
2023

Document Version
Final published version

Published in
Journal of Cultural Heritage

Journal of Cultural Heritage 59 (2023) 10–22

Contents lists available at ScienceDirect

Journal of Cultural Heritage

journal homepage: www.elsevier.com/locate/culher

Original article

Plasters with mixed-in crystallization inhibitors: Results of a 4-year monitoring of on-site application

Barbara Lubelli[a,*], Ernst des Bouvrie[b], Timo G. Nijland[c], Ameya Kamat[a]

[a] Delft University of Technology, Delft, the Netherlands
[b] Independent research, previously affiliated to TU Delft
[c] TNO, Delft, the Netherlands

ARTICLE INFO

Article history:
Received 3 August 2022
Accepted 31 October 2022

Keywords:
Salt crystallization
Crystallization inhibitor
Mortar
Plaster
Sodium ferrocyanide
Sodium chloride

ABSTRACT

Salt crystallization is a major cause of weathering of mortars, including plasters and renders. In the last decade, the use of mixed-in salt crystallization inhibitors in mortars has been proposed as a solution to improve the durability of this material with respect to salt decay. Laboratory characterization and accelerated weathering tests have shown encouraging results. However, data on the long-term behaviour of these mortars when applied on-site were missing until now .

In this research the durability with respect to salt decay of a lime-based plaster and a salt accumulating plaster has been assessed. These plasters, with and without sodium ferrocyanide, a well-known inhibitor of sodium chloride crystallization, have been applied to an interior brick masonry wall with a high salt (sodium chloride) and moisture load and monitored for a period of 4 years.

Monitoring included visual and photographic observations of the damage as well as measurements of the moisture and salt content and distribution, both in the wall and in the plaster. Moreover, the content and distribution of the inhibitor in the plaster after 4 year exposure was measured, to gain insight into the dissolution and transport of the inhibitor.

The results of the research clearly show that the inhibitor is able to significantly reduce the occurrence of salt-induced decay in the lime-based plaster, in comparison to the plaster without inhibitor. No conclusions can be drawn in the case of the salt accumulating plaster, as no decay has developed yet in this case. Two issues related to leaching of the inhibitor and surface discolouration have emerged. These are discussed and possible solutions are proposed.

1. Introduction

Salt crystallization is a major cause of weathering of porous building materials (e.g. [1,2]). Salt decay is often present in old, historic buildings, because of their long-term exposure to moisture and salts. Amongst building materials, plasters and renders are most often suffering of decay due to salt crystallization. There are different reasons for this. First of all, plasters and renders are located at the evaporation surface, where salt accumulate during evaporation. Secondly, their pore size distribution is generally bimodal, with coarse pores (interstitial pores between aggregate and binder) and fine pores (in the binder mass), a fact that is considered having a negative influence on the resistance to salt decay [3]. Finally, the mechanical strength of plasters and renders is generally low, and often unable to withstand salt crystallization pressures.

The low durability of plasters and renders with respect to salt decay results in considerable maintenance and renovation costs. Climate change might intensify the relevance of salt decay [4,5] hence costs. Existing solutions to improve their durability mainly focus on increasing the strength of the material, e.g. by the use of cement binders, and/or on inhibiting salt solution transport (e.g. by the addition of water repellent mixed in the mass [6–8]). However, both these solutions have proven to be not always compatible with existing materials in historic buildings, often worsening the problem they were supposed to solve [6].

In the last decade, an alternative solution has been proposed to improve the durability of lime mortars, and thus also of renders and plasters, with respect to salt decay. This consists in mixing an inhibitor of salt crystallization in the mortar during its preparation. Crystallization inhibitors are ions or molecules which slow down

* Corresponding author at: Delft University of Technology, Faculty of Architecture, Julianalaan 134, Delft, 2628BL Delft, the Netherlands.
E-mail address: b.lubelli@tudelft.nl (B. Lubelli).

https://doi.org/10.1016/j.culher.2022.10.016

nucleation and/or modify crystal growth (see e.g. [9–11]). The application of crystallization inhibitors to the practice of conservation was proposed for the first time about 20 years ago [12,13]. This possibility was then thoroughly investigated in the European project SALT CONTROL [14]: in this research, the effect of inhibitors on crystal growth and salt solution transport was assessed (e.g. [15–18]). One of the tested inhibitors, sodium ferrocyanide, an inhibitor and modifier of sodium chloride [19], was shown to enhance salt transport to the surface during drying, favouring the crystallization of the salts as harmless efflorescence, instead of its precipitation in the pores [17]. The authors attributed this behaviour both to the delayed precipitation of salts, and thus to reduced pore clogging, and to the branched habit of the salts, having a larger evaporation surface than the regular cubic crystal. Moreover, they observed that the inhibitor, in order to be most effective, needs to be present in the material before crystallization of the salt. In a follow-up experiment [20], mortar specimens were contaminated with a watery solution of sodium chloride and sodium ferrocyanide and subjected to dissolution/crystallization cycles of the salt; its behaviour was compared to that of a specimen contaminated with sodium chloride only. This experiment showed that no crystallization-induced dilation was measured in the specimen in which the inhibitor was added and, consequently, no salt crystallization-induced decay occurred. In the years after, the use of different crystallization inhibitors, as method to mitigate salt decay was assessed by several researchers, often with promising results (e.g. [21–26]).

In all the experiments reported above, the inhibitors were added to the materials in aqueous solution. About 10 years ago, the first attempts were made to engineer a mortar in which the inhibitor was mixed-in during preparation, in order to be immediately responsive at the moment a salt solution would penetrate the material. After a promising pilot test [27], an extensive research on lime-based mortars with mixed-in crystallization inhibitor was developed. The effects of the sodium ferrocyanide on the fresh and hardened lime mortar properties were assessed and proven minor [28]. In an accelerated crystallization test, the lime-based mortar with mixed-in inhibitor was shown to have a better resistance to salt decay than the reference mortar [29].

Based on these encouraging results, a research was set-up by the authors in 2018 to assess the durability of mortars with mixed-in inhibitor in the field. The results of this research are reported in this paper.

2. Materials and methods

2.1. Site selection

The selected case study is a church in the province of Zeeland, in the south-western part of the Netherlands. This building was flooded by the sea in 1953, up to its window sills; this resulted in an extremely high salt load in the masonry and a rapid decay of the plaster. After the flooding, the walls were covered with a tar layer, meant to stop the transport of the salt to the surface, and a cement-based plaster layer on top of that. With time, this solution proved ineffective; in a renovation campaign in the 1990′s, both the plaster and tar layer were removed and a new cement-based plaster (classified as “slow transporting plaster” according to [6]) was applied. After a few years, this plaster started showing salt-induced decay, which developed very quickly [30]. Extensive research showed that the decay in the plaster is due to crystallization of sodium chloride, the main salt present in the walls of this building [30,31].

Two types of plaster have been applied, both with and without mixed-in inhibitor. An inner wall in the apse of the church (Fig. 1 left) has been selected as location for their application. The plasters were applied on the two sides of the same wall, to minimize as much as possible differences in external conditions. Each plaster was applied on two adjacent areas, each area being about 1 m wide and 2 m high (Fig. 1 right).

Table 1
Test areas, plaster type and addition of inhibitor.

Test area	Plaster type	Mixed-in inhibitor	
		Inner layer	Outer layer
A1	Lime-based plaster	Yes	Yes
A2	Lime-based plaster	No	No
B1	Cement-based salt accumulating plaster	Yes	No
B2	Cement-based salt accumulating plaster	No	No

Prior to the application, the salt and moisture content in the wall were assessed. The existing plaster (the cement-based plaster applied in the 1990's) was removed and, after wetting of the masonry, the selected plasters were applied.

2.2. Plasters composition and application

Two plaster compositions were tested:

- a lime-based plaster, based on the recipes developed in previous laboratory research [29]. This plaster is made of hydrated lime powder (Supercalco97 by Carmeuse) and quartz sand (grain size between 0.3 and 1 mm), with a binder/aggregate ratio 1:3 in volume. This plaster has been applied in two layers. This plaster was selected as it is expected to have a limited durability to salt crystallization; this would enable the assessment of the effect of the inhibitor within a relatively short period.
- a commercial renovation plaster system, selected as representative of the so-called salt-accumulating plasters (according to the classification proposed in [6]). These plasters are frequently applied on salt laden substrates in renovation interventions. The selected plaster system is composed by two layers: an inner (SanierGrundputz SG 68, Baumiet) and an outer (SanierPutz Fein 64F, Baumiet) layer. According to the information provided by the producer [32,33], the grain size distribution of the two layers is 0 - 4 mm and 0 - 1.2 mm, for the inner and outer layer, respectively; both layers are reported to be based on cement and lime binders, with the addition of unspecified additives. No exact values are reported for water absorption; however, the indicative properties reported in the product information sheet suggest that the inner layer has a higher water absorption by capillarity than the outer layer. This is common in salt accumulating plasters and renders, in which the inner layer is meant to accumulate the salt and the outer layer to inhibit the transport of salt to the surface.

Sodium ferrocyanide ($Na_4[Fe(CN)_6 \bullet 10H_2O$, Sigma Aldrich) was used as an inhibitor to be added to the plaster. Each plaster was prepared with and without the addition of the inhibitor. In the case of the lime-based plaster, the inhibitor was added in both the inner and outer layer of the plaster. In the case of the renovation plaster, the inhibitor was added to the inner layer only; this was done as salts are not supposed to reach the outer layer of the plaster, because of the working principle of salt accumulating plasters (Table 1).

In both cases, the inhibitor was dissolved in the water used for mixing the plasters, in an amount equal to about 1% of the weight of the binder. In order to ensure that the entire amount of inhibitor would be incorporated in the plaster, the inhibitor was dissolved in an amount of water lower than that necessary to obtain a workable mortar; additional water was then added until a good work-

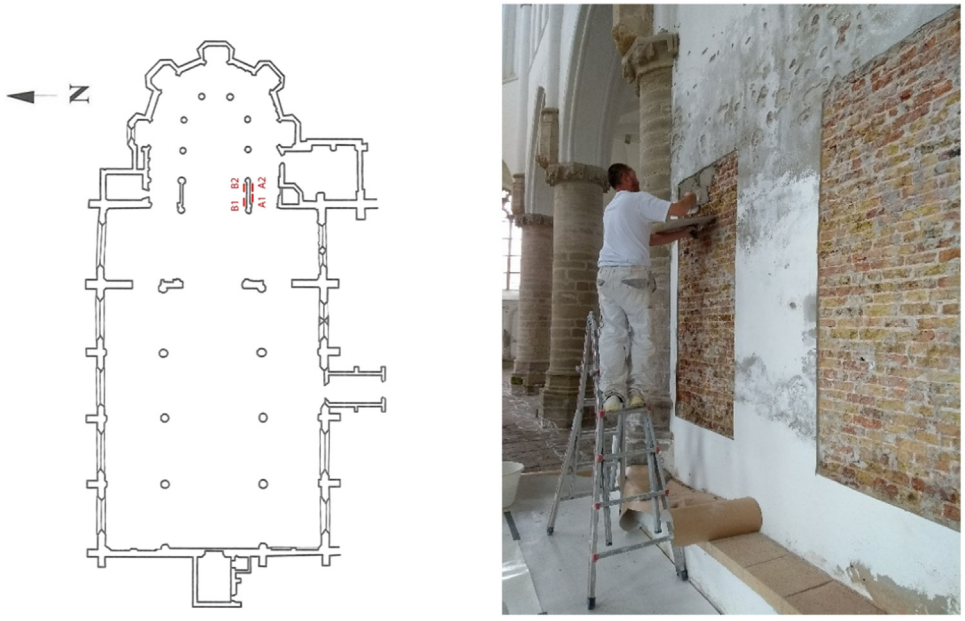

Fig. 1. Left: Plan of the church with indication of the location of the test area; Right: application of the plaster on the test area.

ability was reached. The first layer of both plasters was applied in a thickness of about 18 mm. After 2 weeks, the second layer, with thickness of about 10 mm, was added on top. The thickness of the plaster varied a bit from place to place, because of the irregular surface of the wall.

2.3. Plaster characterization methods

Characterization tests were carried out on both plasters. As it is known that the mortar properties can be significantly affected by the properties of the substrate on which they are applied [34], the properties of the plasters were measured on cores sampled from the test panels.

About 4 months after the application, several cores of about 50 mm diameter were drilled in the plasters, at about the same height from the floor. It was not always possible to drill the cores without the use of water. Care was taken to limit the amount of water, in order to avoid as much as possible dissolution of the salts. Cores which were drilled dry were selected for microscopy observations, so that it would still be possible to distinguish salt crystals in pores, if present. All cores were dried in an oven at 40 °C until they reached a constant weight, before testing them. The water absorption by capillarity of the salt accumulating plaster was measured on each single layer.

Prior to the water absorption test, the lateral surface of the cores was sealed with epoxy resin, impermeable to liquid water and water vapour. Demineralized water was poured in a container, on the bottom of which a grid was placed. The bottom surface of the cores, corresponding to the surface of the plaster originally in contact with the masonry, was placed on the grid and immersed in water up to 2 mm from the bottom surface; the water level was kept constant during the test. The weight of the specimens was recorded at regular time intervals. Once the samples reached a constant weight, they were immersed under water for 24 h. Afterwards, their weight in air and in water was measured and their density calculated as follows [35]:

$$\text{Total water absorption [w\%]} = 100 * \frac{(\text{saturated weight in air} - \text{dry weight})}{\text{dry weight}} \quad (1)$$

$$\text{Density}\left[\text{kg/dm}^3\right] = \frac{(1000 * \text{dry weight})}{(\text{saturated weight in air} - \text{saturated weight in water})} \quad (2)$$

Polarizing and fluorescence microscopy (PFM) observations were carried out on thin sections of both plasters, with and without inhibitor, with the aim of assessing the composition of the salt transporting plaster and possible differences in structure between the plasters with and without inhibitor.

The cores were first impregnated with epoxy resin; subsequently, thin sections of the thickness of 25- 30 µm were prepared; no water was used for cutting and polishing the thin sections, to avoid dissolution of the salts possibly present in the material.

2.4. Monitoring

The state of conservation of the test panels was visually and photographically recorded at 3, 6, 12, and 48 months after the application.

Additionally, the moisture and salt content in the wall and in the plasters were determined, before the application (t0) and at 3 (t3) and 48 (t48) months after the application. To this scope, powder samples were collected on all panels at different depths and heights, in the plaster and in the masonry underneath up to 20 cm depth, along a vertical profile. The moisture content (MC) of the samples was determined gravimetrically, after drying of the samples at 40 °C, in the following way:

$$\text{MC} = 100 * \frac{\text{weight sample} - \text{dry weight sample}}{\text{dry weight sample}} \quad (3)$$

The salt content in the samples was indicatively assessed by storing them for 4 weeks at 20 °C at 95% RH and measuring their hygroscopic moisture content (HMC) as follows: selectfont

$$\text{HMC} = 100 * \frac{\text{weight sample after storage at 95\%RH} - \text{dry weight sample}}{\text{dry weight sample}} \quad (4)$$

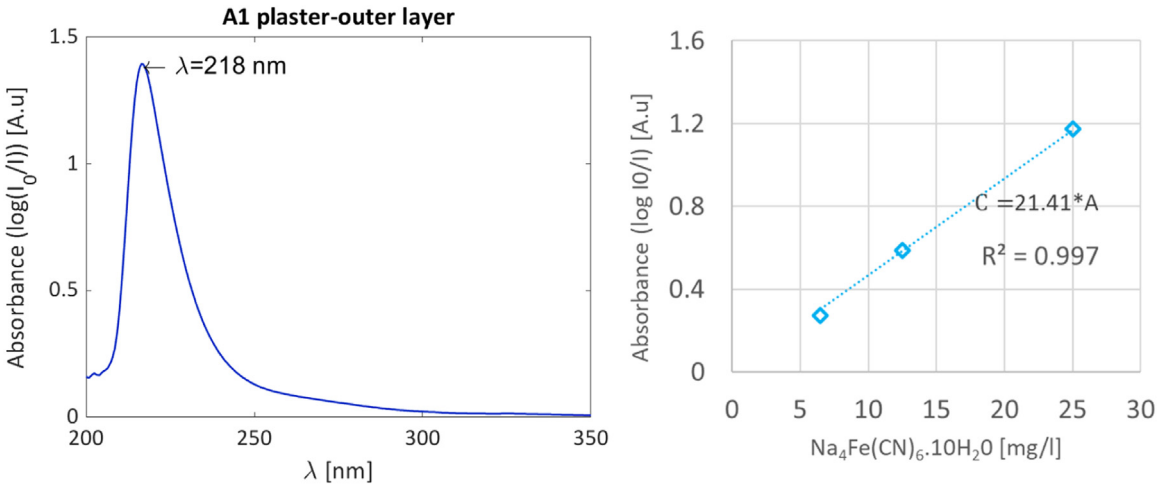

Fig. 2. Left: Example of the spectroscopic result for a plaster sample with inhibitor (panel A1); Right: Calibration showing concentration as a function of absorbence for sodium ferrocyanide ions.

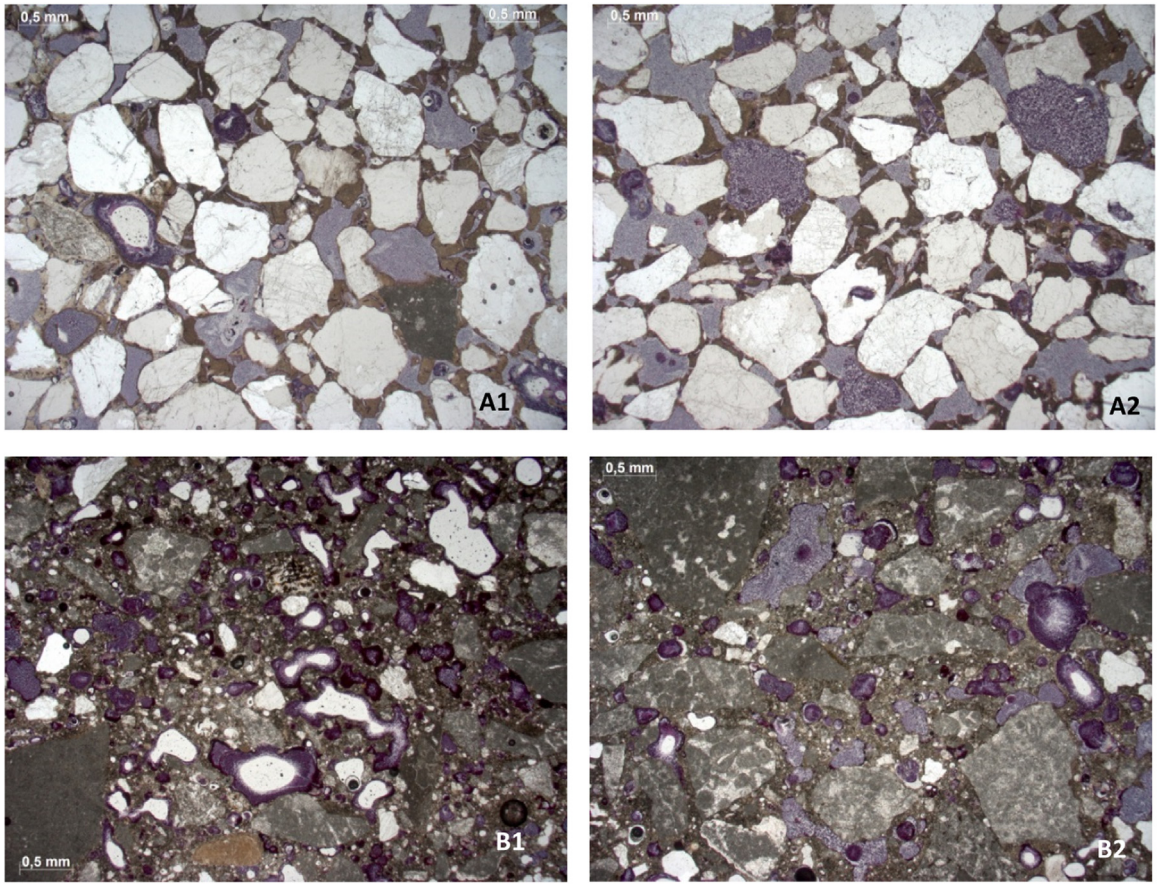

Fig. 3. Microphotographs with an overview of the microstructure of the lime based plaster with (test panel A1, top left) and without inhibitor (test panel A1, top right) and the inner layer of the salt accumulating plaster with (test panel B1, bottom left) and without inhibitor (test panel B2, bottom right) (parallel polarized light).

The HMC gives a reliable indication of the presence of hygroscopic salts in the samples [36–39].

The presence and distribution of the inhibitor in the plaster was assessed in order to determine the relevance of leaching and transport of the inhibitor to the surface of the wall. Samples collected at t48 from the inner and outer plaster layer of panel A1 and B1 were analysed; additionally, some plaster samples collected from areas of panel A1, with and without blue discolouration, were analysed to check the relation between the amount of inhibitor and the observed change in colour.

The content of inhibitor in plaster samples was measured using UV–VIS spectroscopy (Shimadzu UV2600). The samples for UV–VIS were prepared by first grinding 500 mg of the oven-dry plaster sample using a pestle and a mortar, and subsequently adding them

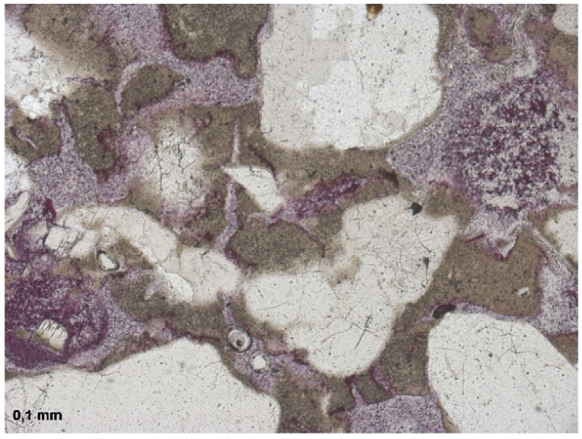

Fig. 4. Microphotograph showing a detail of the lime based plaster without inhibitor, where many shrinkage cracks are visible (parallel polarized light).

to 30 ml of deionised water. The powder samples were then thoroughly shaken and stored overnight to allow for dissolution of the inhibitor. The solution was then passed through a Whatman size 1 filter, in order to obtain a clear solution, necessary for the UV–VIS analysis.

An example of the spectroscopic data is presented in Fig. 2 left. A characteristic peak is observed at a wavelength of 218 nm due to the presence ferrocyanide ions $(Fe(CN_6)^{4-}$ and corresponds well with the data from the literature [40].

The intensity of the absorbence (A) measured by the detector follows the Beer-Lambert law and is directly proportional to the concentration (C) dissolved in the solutions, as shown in Eq. (5) [41] The terms I_0 and I correspond to the incident and the transmitted light intensity respectively.

$$A = \log_{10}\left(\frac{I_0}{I}\right) = k \cdot C \tag{5}$$

A calibration was performed to obtain the value of k. For calibration, 3 standard solutions containing inhibitor in ultra-pure water were analysed for absorbence with an inhibitor concentration of 25 mg/l, 12.5 mg/l and 6.25 mg/l. The k value was determined using linear regression without an intercept term to stay true to Eq. (5). Ultra-pure demi water was used as a reference specimen and all specimens were measured in standard 5 ml cuvettes with the same path length of 1 cm. Spectroscopic data was acquired for wavelengths between 350 nm and 200 nm and the absorbence obtained at 218 nm was used for quantitative analysis. The calibration curve for the UV–VIS quantitative analysis is presented in Fig. 2 right. A good correlation is obtained between the absorbence and the sodium ferrocyanide concentration in the solution.

The presence of Fe^{3+} ions in the brick of the masonry wall was qualitatively assessed by making use of 1.25% w/v potassium thiocyanate (KSCN) as an indicator. The samples were prepared by mixing 0.5 g of finely ground brick with 30 ml of deionised water. The samples were further acidified with concentrated hydrochloric acid (HCl) to reach pH 1. This step was necessary to dissolve any iron related products (e.g. Fe_2O_3), otherwise insoluble in water, and to oxidize Fe^{2+} to Fe^{3+}ions. The sample was further passed through a medium speed filter (Whatman No. 40) to separate the debris and obtain a clear solution. The clear solution was tested for Fe^{3+} ions by adding a few drops of KSCN. Presence of Fe^{3+}can be confirmed by the change in colour of the solution from colourless to red as per Eq. (6) [42].

$$Fe^{3+} + 3SCN^- \leftrightharpoons Fe(SCN)_3 \text{ (red)} \tag{6}$$

3. Results

3.1. Microscopy observations

The microscopy observations on the thin sections of the lime-based plaster show that this plaster has a homogenous microstructure, with numerous compaction voids; entrapped air void are rare (Fig. 3- A1 and A2) and only a few shrinkage cracks occur (Fig. 4). No relevant differences in the microstructure could be observed between the lime-based plaster with and without inhibitor (compare Fig. 3- A1 and A2). This is in line with the results of previous research [28].

The microscopy observations on the thin sections of the salt accumulating plaster (Fig. 3- B1 and B2) show that the binder of both layers is the same and it consists of Portland cement (CEM I) with the addition of lime. This confirms what reported in the product information sheet. The aggregate consists of crushed limestone, some quartz sand and a light weight aggregate (expanded clay); the latter is more abundant in the outer layer (Fig. 5). The porosity of the inner layer is higher and coarser than that of the outer layer, results which confirm the indicative data reported in the information sheet. No shrinkage cracks are observed in any of the layers. Also in this case, as observed for the lime-based plaster, no differences are visible in the microstructure of the plaster with and without inhibitor

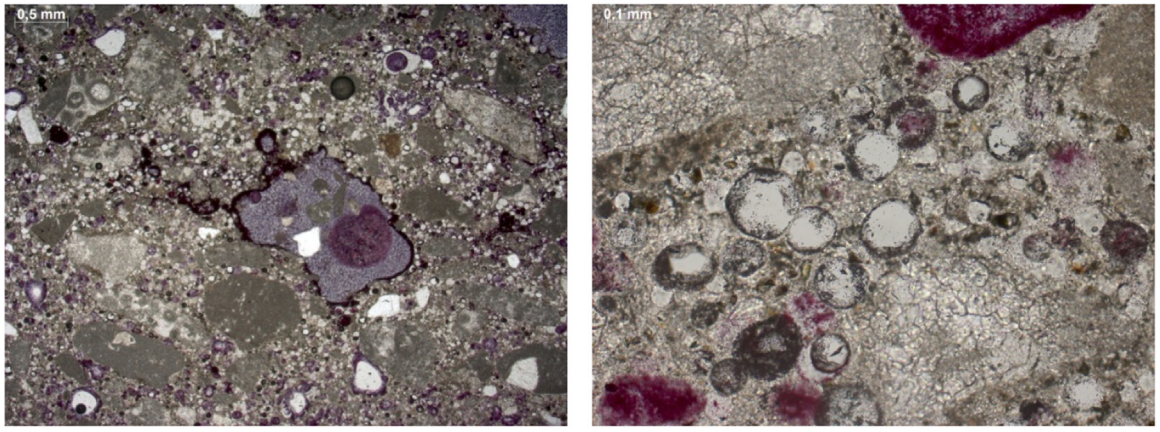

Fig. 5. Microphotographs with an overview (left) and detail (right) of the microstructure of the outer layer of the salt accumulating plaster in which the light weigh aggregate is visible (parallel polarized light).

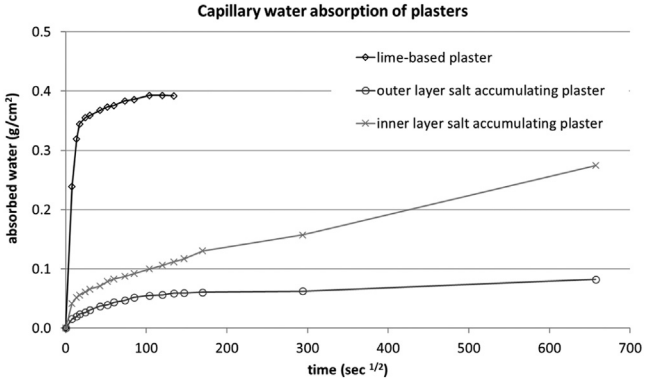

Fig. 6. Water absorption by capillarity of the plasters.

3.2. Moisture transport properties of the plasters

The water absorption by capillarity of the plasters is shown in Fig. 6. As expected, the lime-based plaster shows the fastest water absorption rate. The outer layer of the salt accumulating plaster has the lowest absorption rate; however, the plaster is still able to absorb water. The low water absorption rate of the outer layer can be due to the presence of additives reducing the water transport and/or the presence of a large amount of coarse and partially closed pores in the light weight aggregate, which has a delaying effect on capillary transport (very coarse pores can hardly suck water from the smaller pores present in the binder).

The lime-based plaster shows a higher density (1791 kg/dm^3) than the outer (1350 kg/dm^3) and inner (1591 kg/d m^3) layer of the renovation plaster: this is most probably due to the presence the light weight aggregate in the renovation plaster.

3.3. Visual and photographic monitoring of decay on site

The test panels were inspected several times in the 4 years after the application (Fig. 7). Three months after the application (t3), blue spots were visible in the lower part of panel A1 (lime mortar with inhibitor), while a yellow discolouration was distinguishable over the entire panel; the intensity of both colours increased with time. The yellowish colour is most probably caused by the inhibitor itself (sodium ferrocyanide is pale yellow). Alternatively, the yellowish colour may be due to oxidation of ferrocyanide to ferricyanide under influence of UV light [43], which subsequently oxidixes to Fe-hydroxide. The blue discolouration is most probably the result of reaction of ferrocyanide ions with Fe^{2+} or Fe^{3+} in solution, resulting in the formation of Trumbull's blue ($Fe_3[FeCN_6]_2$ or Prussian blue ($Fe_4[FeCN_6]_3$), respectively, both a blue pigment [44]. The corresponding panel A2 shows no colour change; with time, starting from months 6, some moist spots appeared on the surface in the lower part of this panel.

Three months after the application, some efflorescences appeared in the lower part of panel A1. Their amount increased after 12 months. The salt crystals showed a dendritic form and could be brushed off very easily (Fig. 8 left); both these characteristics are typical for NaCl crystallizing in the presence of a ferrocyanide inhibitor. [29] [45] On panel A2, efflorescences appeared only after 6 months. In this case, the salts were adherent to the surface and could not easily be brushed off (Fig. 8 right).

Decay, in the form of loss of cohesion (sanding), was observed in panel A2, between 120 and 170 cm height, 48 months after the application of the plaster. In contrast, no loss of cohesion is observed in panel A1 up to 48 months (Fig. 9).

Panels B1 and B2 did not show any damage 48 months after application; no efflorescences were observed at the surface. In the case of panel B1, 48 months after the application, a very slight blue discolouration was visible at some spots (Fig. 7).

As mentioned above, the blue discolouration is most probably due to formation of Trumbull's blue ($Fe_3[FeCN_6]_2$ or Prussian blue ($Fe_4[FeCN_6]_3$). For this reaction to occur the presence of Fe^{3+} is necessary. In this case, the brick in the masonry beneath the plaster is a possible source of Fe^{3+}. In order to validate this hypothesis, a simple, qualitative assessment of the presence of Fe^3 in the brick was carried out, according to the method described in § 2.4. The addition of KSCN changed the colour of the solution from colourless to red, indicating presence of Fe^{3+} ions (Fig. 10) .

3.4. Moisture and hygroscopic moisture distribution

The moisture content (MC) and hygroscopic moisture content (HMC) distribution measured before the application of the plasters (t0) are reported in Fig. 11. At the bottom of the wall, a high moisture content is measured, which decreases with height and increases with depth. A high HMC is measured near the surface of the wall, in the old plaster layer; the highest HMC values are measured in the upper part of the wall.

Based on the MC and HMC results, it can be concluded that rising damp from ground water is present, up to a height of 1.5–2 m from the floor. Higher up in the wall, the measured moisture content is mainly due to the presence of hygroscopic salts, in combination with the relative humidity of the air in the church [31][30]. Salt accumulation is observed at 300 cm, higher than the current maximum height of the rising damp. Two factors have possibly contributed to this: the flooding in 1953 (the church was flooded up to its window sills, located at about 2.5 m) and the use of a tar layer during the renovation works in the 1950′s, inhibiting evaporation and thus increasing the height reached by rising damp.

Despite all test areas are located on the same wall, some differences in moisture and salt content and distribution occur amongst them. Such differences are not unusual in old buildings. In this case, they may be due to previous renovation interventions (e.g. possible incomplete removal of the tar layer in the 1990′s) or due to differences in the properties of the bricks used in the masonry.

The MC in the masonry beneath the plaster layer before (t0), at 3 months (t3) and 48 months (t48) after the application of the new plasters is reported in Fig. 12. The MC in the masonry varies considerably in time. Despite these variations, the MC in the lower part of the wall is always much higher than in the upper part, and it increases with depth. This confirms once again the presence of rising damp in the wall. Variations in the MC are most probably due to (seasonal) changes in ground water level and to differences in the properties of the sampled materials, as it was not always possible to collect samples in the same brick/mortar joint.

The HMC measured in the wall 48 months after application of the plaster is reported in Figs. 13 and 14. The HMC in the plaster in panels A1 and A2 indicates that significant transport of salt solution has taken place from the masonry to the plaster layer, at all heights in the wall. This is in agreement with the quick moisture transport measured for this plaster. Besides, it can be observed that the MC influences the location of the salt accumulation: in the lower part of the wall, where the MC in the wall is higher, salts are transported easier towards the surface and accumulate in the outer part of the plaster; in the upper part of the wall, where the MC is lower, salts accumulate in the inner part of the plaster.

It is hard to draw conclusions on the effect of the inhibitor on the amount of salts in the plaster. Differences in salt content in the plaster in A1 and A2 are mainly due to differences in the salt content in the masonry beneath. However, it is possible to confirm that the inhibitor increases the resistance of the plaster to salt de-

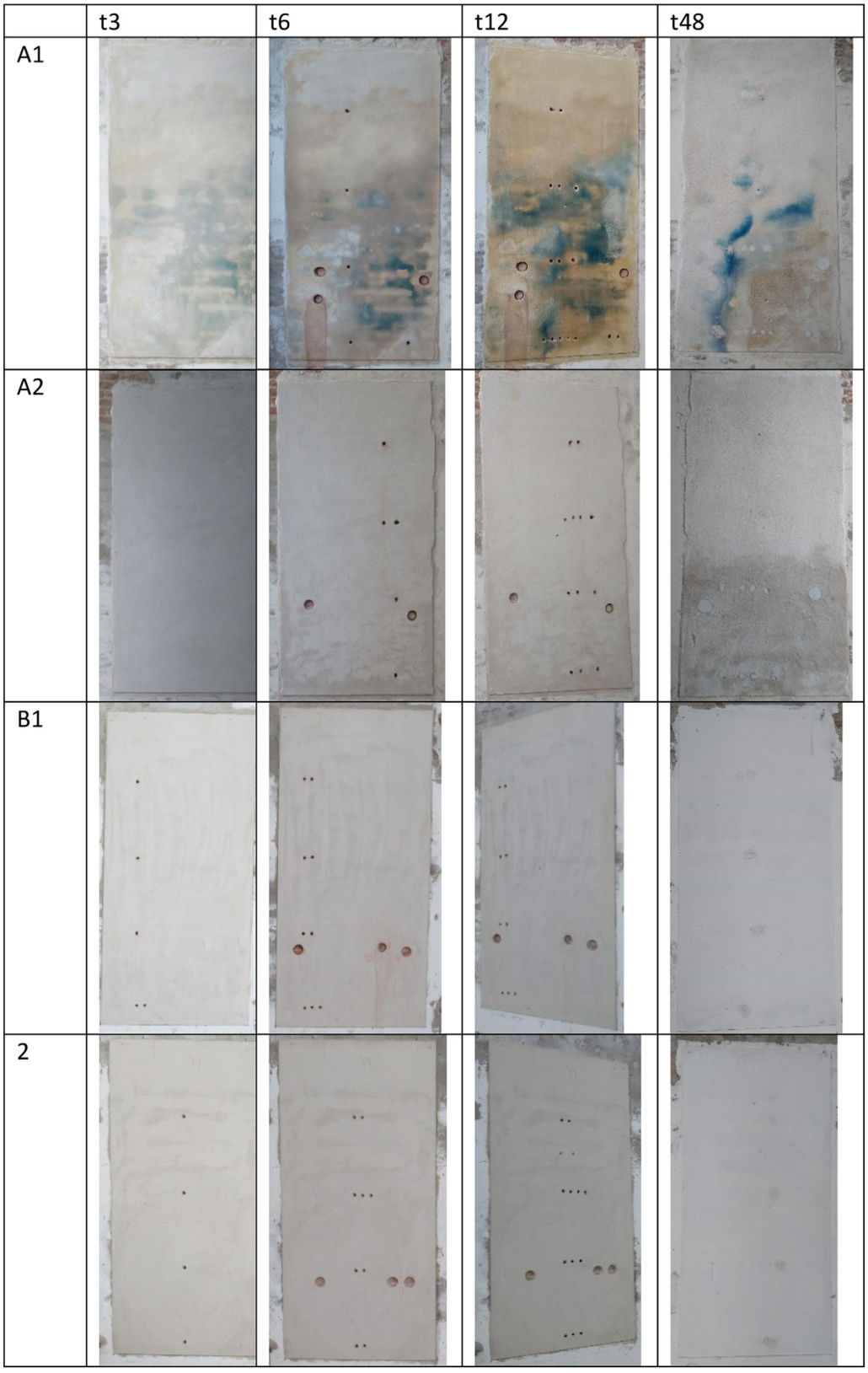

Fig. 7. Panels A1, A2, B1 and B2, after 3 (t3), 6 (t6), 12 (t12), 39 (t39) and 48 (t8) months after the application (a white paint was applied on the surface of the panels in the period between t12 and t48).

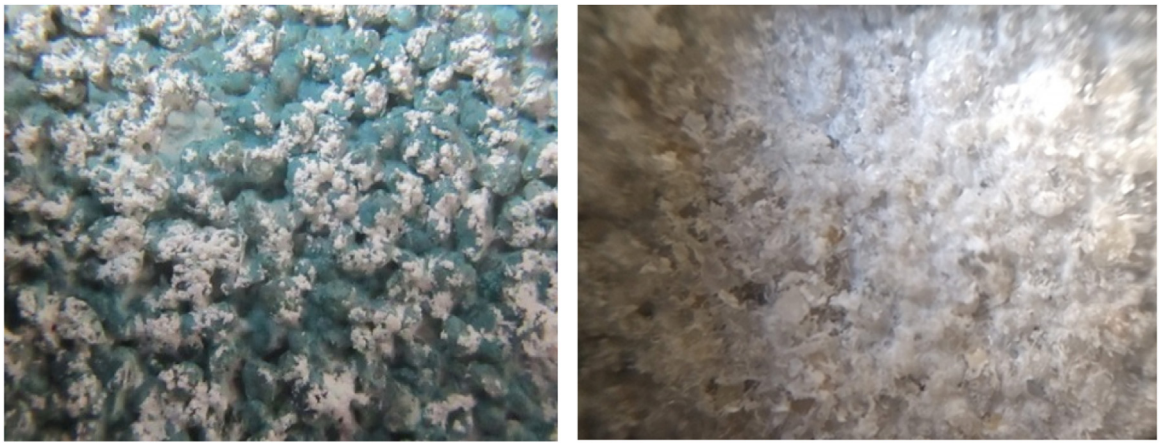

Fig. 8. Left: Dendritic salt efflorescence on panel A1, 3 months after the application; Right: salt crust on the surface of panel A2, 6 months after the application (right).

Fig. 9. Left: Panel A1: No loss of cohesion of the plaster; Right: Panel A2 significant sanding of the plaster; Situation 48 months (t48) after the application.

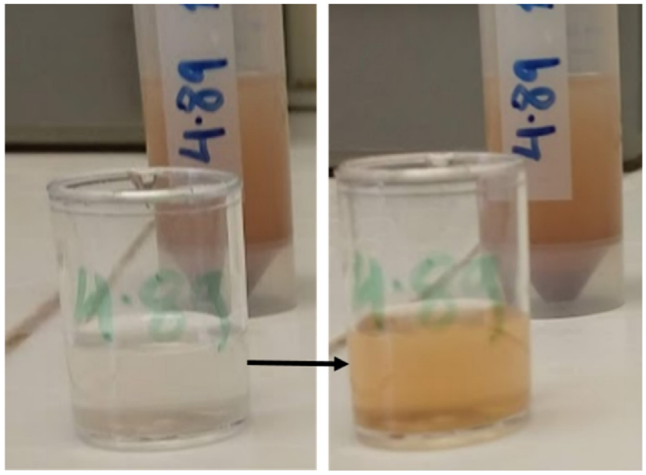

Fig. 10. Left: acidified clear solution from the bricks before addition of the indicator. Right: change in colour from colourless to red on addition of the indicator, detecting the presence of Fe^{3+} ions.

cay: in fact, at 100 cm and 150 cm height, panel A1 shows no decay whereas panel A2 suffers of loss of cohesion, despite panel A1 has a comparable (at 150 cm height) or even higher (at 100 cm height) salt content than panel A2.

The HMC distribution in the plaster of panels B1 and B2 shows that salts have been transported into the plaster. Similarly to what observed for panels A1 and A2, at lower heights (100 cm), where the moisture content in the masonry is very high, salts have been transported more towards the surface; though, no efflorescences are present in this case. Higher up in the wall, where the moisture content in the masonry is lower, salts have accumulated in the inner layer, as expected for this plaster type. The HMC in the plaster is higher in panel B1 than in panel B2; however, also in this case, it is not possible to draw definitive conclusions on the effect of the inhibitor on the salt transport, as the differences in salt content in the plasters can be due to differences in salt content in the masonry beneath.

3.5. Distribution of the inhibitor

The distribution of the inhibitor in the outer and inner plaster layers of panels A1 and B1 is reported in Fig. 15. The results are normalized and expressed as the amount of inhibitor present (mg) per mass of the plaster specimen (g).

In the lime-based plaster of panel A1, the highest amount of inhibitor is found in the lower part of the wall, at heights of 100 and 150 cm, in the outer layer of the plaster. The higher concentration of the inhibitor in the outer layer can be explained by the high moisture content in the wall at this height, favouring the

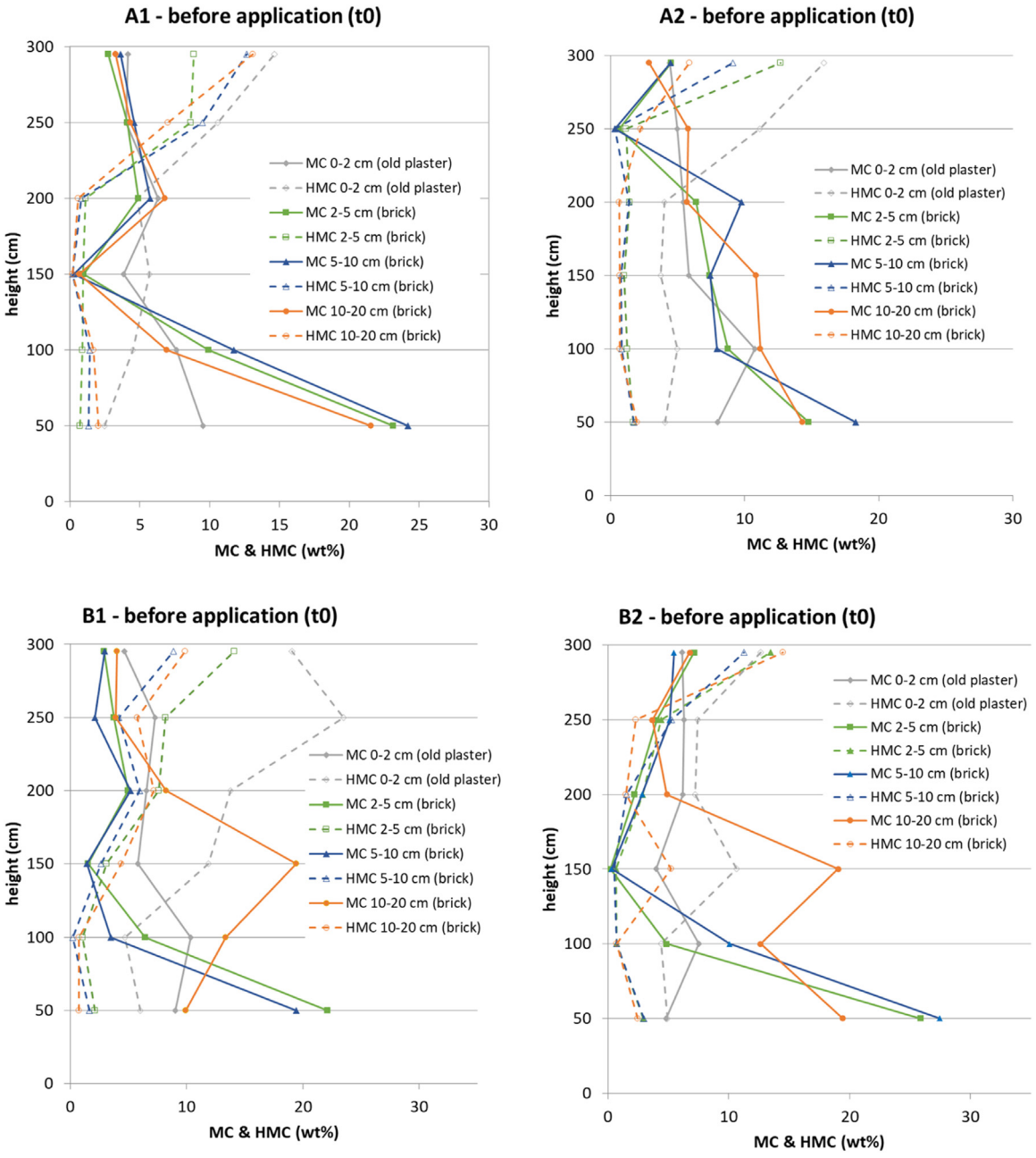

Fig. 11. MC and HMC distributions in the test areas before the application of the plasters (t0).

dissolution and transport of the inhibitor towards the evaporation surface. The inhibitor amount decreases with height, in both the outer and the inner layer. The reason of this is unclear: differences in the thickness of the plaster layer, and thus in the total amount of available inhibitor at the different locations, in combination with the high moisture content in the lower part of the wall, enabling transport of the inhibitor to the surface, might explain these results.

In the salt accumulating plaster of panel B1, the amount of inhibitor is generally higher in the inner layer than in the outer layer. This was expected, both because the inhibitor was added only to the inner layer and because the outer layer has a low capillary absorption rate, meant to limit moisture (and thus also salt and inhibitor) transport to the surface. Only in the lower part of the wall (100 cm), where the moisture content in the wall is constantly high due to rising damp, part of the inhibitor has been transported into the outer layer.

When comparing samples from panel A1, it can be observed that the sample collected in the area with blue discolouration contained 2.5 mg/g of inhibitor, almost 2.7 times the amount measured in the sample collected in the non-discoloured zone (0.9 mg/g). Thus, probably, a high ferrocyanide concentration at the surface is necessary in addition to the Fe^{3+} ions to cause a blue discolouration in the plaster.

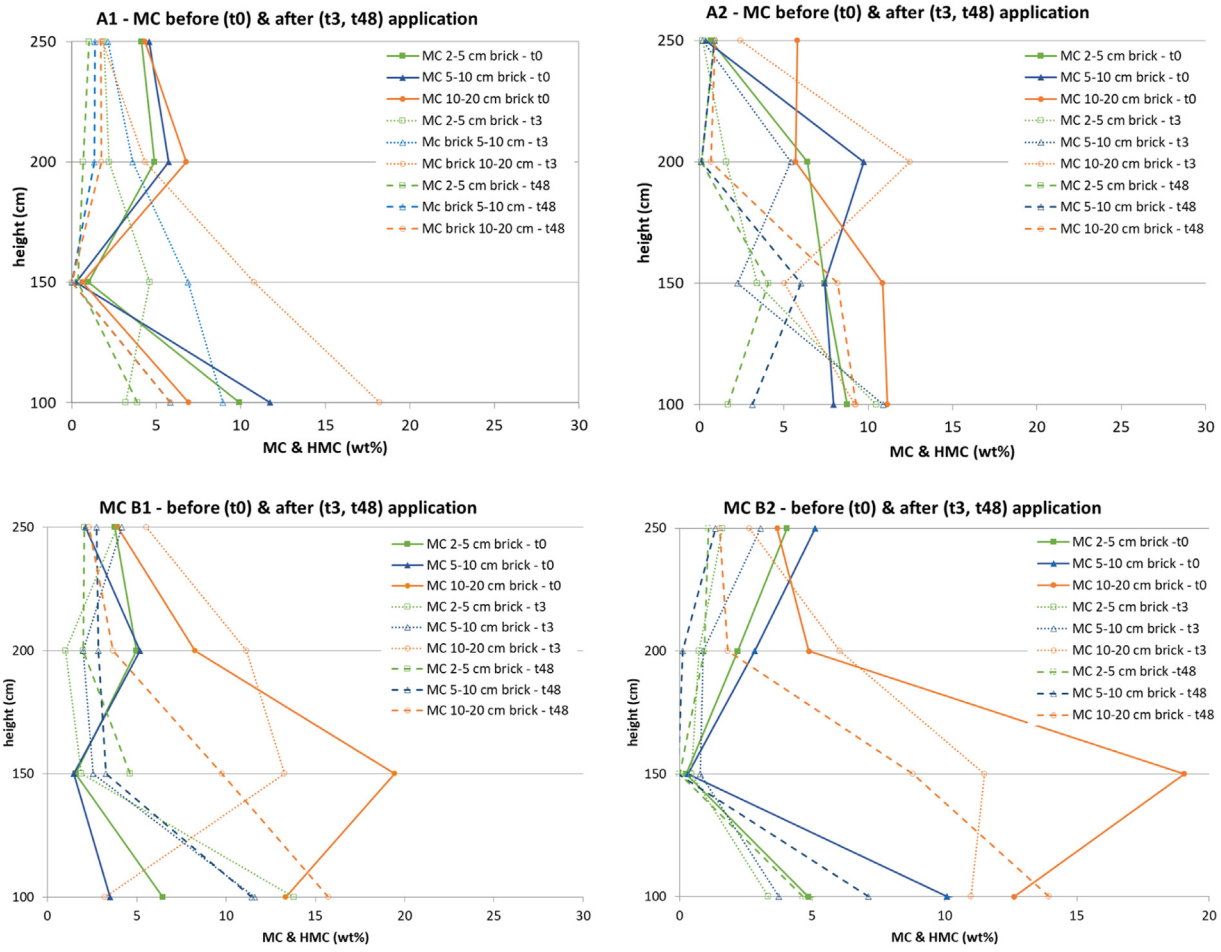

Fig. 12. MC in the test areas before (t0) and 3 (t3) and 48 months (t48) after the application of the new plasters (t48).

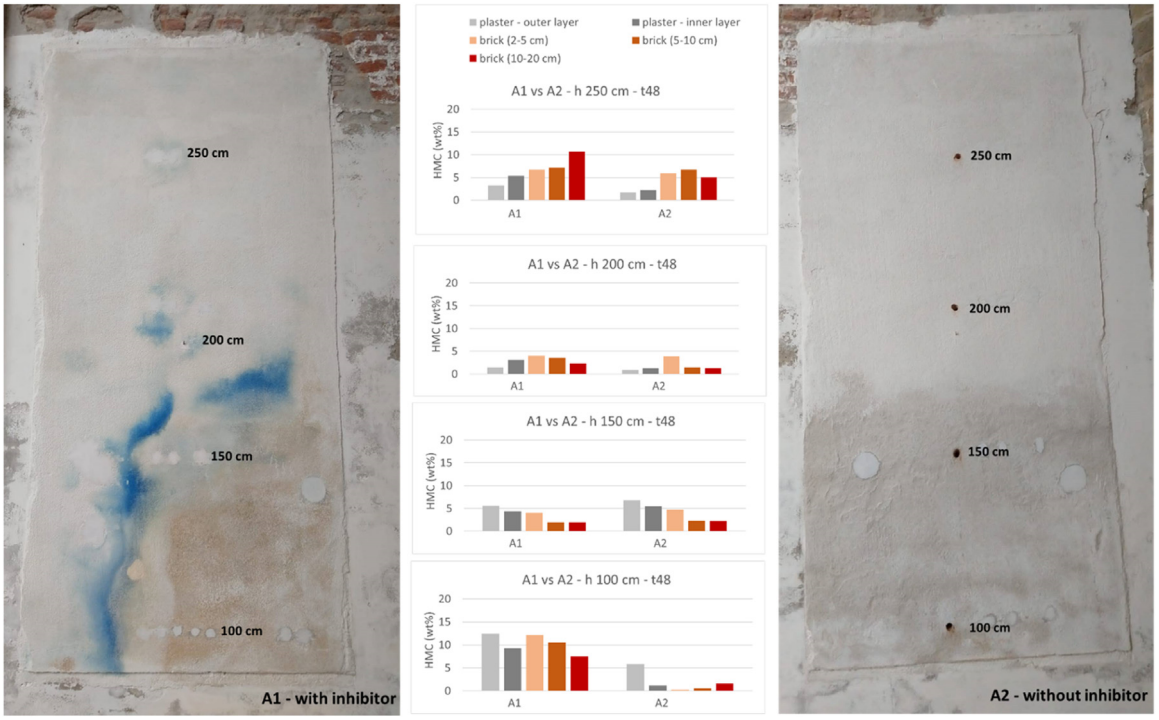

Fig. 13. HMC distribution in test areas A1 (left) and A2 (right) 48 months after the application of the lime-based plaster.

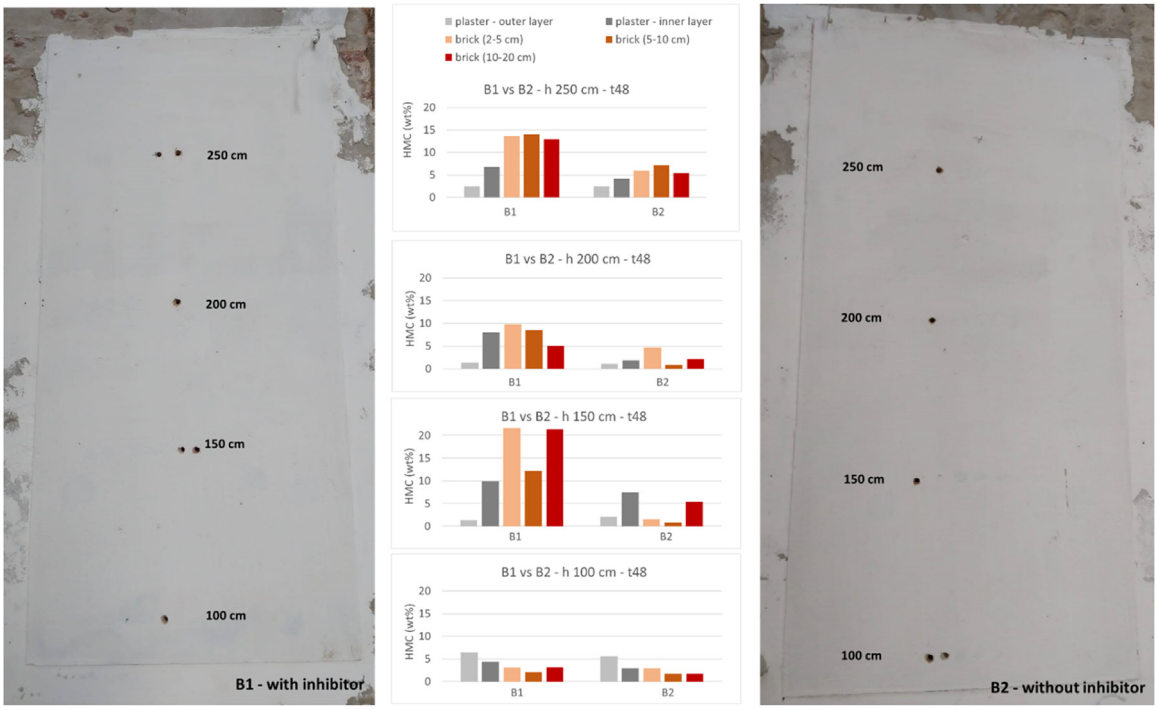

Fig. 14. HMC distribution in test areas B1 (left) and B2 (right) 48 months after the application of the salt accumulating plaster.

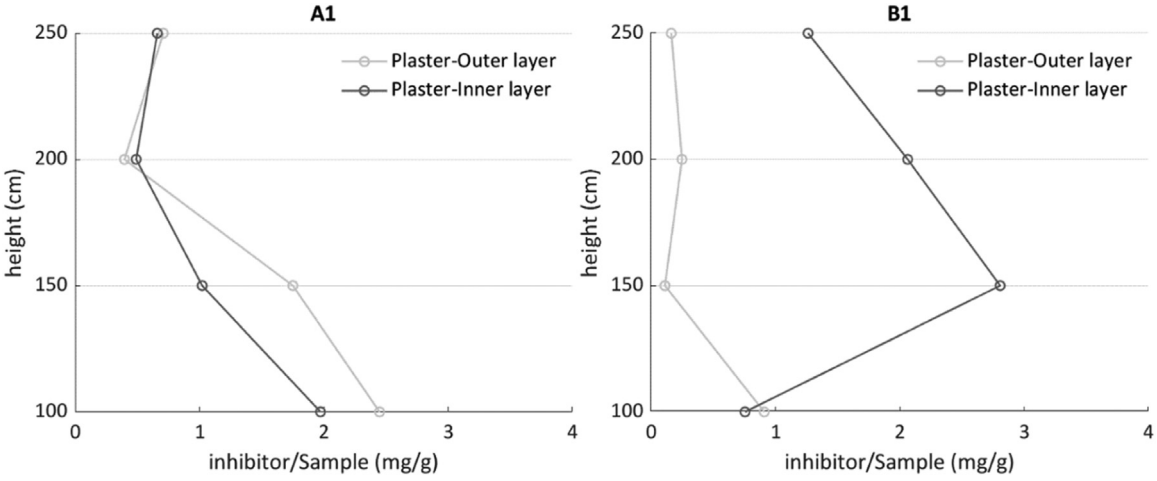

Fig. 15. Inhibitor content and distribution in the plaster in panel A1 (left) and B1 (right).

4. Discussion and conclusions

This paper reports the results of a long-term monitoring of the behaviour of mortars with salt crystallization inhibitors applied on-site. The durability with respect to salt decay of a lime-based plaster and a salt accumulating plaster, both with and without the addition of a salt crystallization inhibitor (sodium ferrocyanide) in the mass, has been assessed. The plasters have been applied to an interior brick masonry wall with a high salt (sodium chloride) and moisture load.

Four years after the application, it can be concluded that the inhibitor is able to reduce the occurrence of salt decay in the lime-based plaster. In fact, loss of cohesion of the surface (sanding) occurs in the lime plaster without inhibitor, whereas no damage is observed in the lime plaster with the inhibitor, despite the comparable moisture and salt content present in the masonry wall. The salt accumulating plaster, both with and without inhibitor, does not show any damage yet.

This clear positive effect of the inhibitor on salt-induced decay confirms the promising results obtained in previous experimental research in laboratory [27,29].

However, two issues have emerged in this study, which need to be tackled in future research. The first issue is related to leaching of the inhibitor. Because of the presence of moisture in the wall, the inhibitor has been dissolved and transported towards the evaporation surface. If the inhibitor accumulates only at the surface, its effect will be limited; besides, it can be removed e.g. with the efflorescences or washed away by rain. A solution for excessive

leaching could be provided by encapsulation the inhibitor and thus controlling its release. Research on this subject is on-going at the moment.

The second issue is the blue discolouration observed on the lime plaster containing the inhibitor, due to formation of Trumbull's blue or Prussian blue from a reaction of ferrocyanide ions with Fe^{2+} or Fe^{3+} in solution. These ions could have been provided by the brick, as the KSCN test shows. Alternatively, it may be speculated that UV-induced photocatalytic degradation of ferrocyanide [43] at the surface resulted in liberation of Fe ions, that subsequently reacted with the ferrocyanide below the surface (in solution).

Encapsulation of the inhibitor, by delaying its release, would also help to slow down discolouration. Besides, the addition of binders with a darker colour than hydrated lime, such as cement, may reduce the visual impact of the discolouration. Another possible solution to this problem consists in adding the inhibitor to the inner layer of salt accumulating plaster, inhibiting its transport to the surface by the use of an outer layer with a low moisture transport capacity. In this study, this solution (panel B1 and B2) has been shown to reduce discolouration, but the positive effect of the inhibitor on salt-induced decay needs to be verified further, by longer monitoring of the test panel and/or by accelerated crystallization tests in laboratory.

Acknowledgments

This research was in part financed by the Cultural Heritage Agency of the Netherlands. The authors wish to thank prof. Rob van Hees for his contribution to the set-up of the research, ir. Hans Dalderop (Eindhoven University of Technology, the Netherlands) for his help with the UV–Vis measurements and colour indicator method, Anton van Delden (Fa Delstuc bv) for the application of the plaster on site and Nico Karper (Strikolith B.V.) for providing the material.

Supplementary materials

Supplementary material associated with this article can be found, in the online version, at doi:10.1016/j.culher.2022.10.016.

References

[1] A. Goudie, H. Viles, Salt Weathering Hazards, Wiley & Sons, 1997.
[2] A.E. Charola, C. Bläuer, Salts in masonry: an overview of the problem, Restor. Build. Monum. 21 (2015) 119–135, doi:10.1515/rbm-2015-1005.
[3] R. Rossi-Manaresi, A. Tucci, Pore structure and the disruptive or cementing effect of salt crystallization in various types of stone, Stud. Conserv. 36 (1991) 53–58.
[4] C.M. Grossi, P. Brimblecombe, B. Menéndez, et al., Climatology of salt transitions and implications for stone weathering, Sci. Total Environ. 409 (2011) 2577–2585, doi:10.1016/j.scitotenv.2011.03.029.
[5] T.G. Nijland, O.C.G. Adan, R.P.J. Van Hees, B.D. Van Etten, Evaluation of the effects of expected climate change on the durability of building materials with suggestions for adaptation, Heron 54 (2009) 37–48.
[6] C. Groot, R. van Hees, T. Wijffels, Selection of plasters and renders for salt laden masonry substrates, Constr. Build. Mater. 23 (2009) 1743–1750, doi:10.1016/j.conbuildmat.2008.09.013.
[7] W. Brachaczek, The hydrophobicity of renovation plaster in manufacturing technology optimized by statistical methods, Constr. Build. Mater. 49 (2013) 575–582, doi:10.1016/j.conbuildmat.2013.08.051.
[8] L. Falchi, E. Zendri, E. Capovilla, et al., The behaviour of water-repellent mortars with regards to salt crystallization: from mortar specimens to masonry/render systems, Mater. Struct. Constr. 50 (2017) 1–15, doi:10.1617/s11527-016-0891-8.
[9] C. Rodriguez-Navarro, L.G. Benning, Control of crystal nucleation and growth by additives, Elements 9 (2013) 203–209, doi:10.2113/gselements.9.3.203.
[10] S.J.C. Granneman, B. Lubelli, R.P.J. van Hees, Mitigating salt damage in building materials by the use of crystallization modifiers – a review and outlook, J. Cult. Herit. 40 (2019) 183–194, doi:10.1016/j.culher.2019.05.004.
[11] M.P. Bracciale, S. Sammut, J. Cassar, et al., Molecular crystallization inhibitors for salt damage control in porous materials : an overview, Molecules 25 (2020) 1873.
[12] C. Selwitz, E. Doehne, The evaluation of crystallization modifiers for controlling salt damage to limestone, J. Cult. Herit. 3 (2002) 205–216, doi:10.1016/S1296-2074(02)01182-2.
[13] C. Rodriguez-Navarro, L. Linares-Fernandez, E. Doehne, E. Sebastian, Effects of ferrocyanide ions on NaCl crystallization in porous stone, J. Cryst. Growth 243 (2002) 503–516, doi:10.1016/S0022-0248(02)01499-9.
[14] SALT CONTROL - EU Project n° 501517 (Contract SSP1-CT-2003-501571) Prevention of salt damage to the built cultural heritage by the use of crystallisation inhibitors
[15] E. Ruiz-Agudo, J.D. Martín-Ramos, C. Rodriguez-Navarro, Mechanism and kinetics of dehydration of epsomite crystals formed in the presence of organic additives, J. Phys. Chem. B 111 (2007) 41–52, doi:10.1021/jp064460b.
[16] E. Ruiz-Agudo, C. Rodriguez-Navarro, E. Sebastián-Pardo, Sodium sulfate crystallization in the presence of phosphonates: implications in ornamental stone conservation, Cryst. Growth Des. 6 (2006) 1575–1583, doi:10.1021/cg050503m.
[17] B. Lubelli, R.P.J. van Hees, Effectiveness of crystallization inhibitors in preventing salt damage in building materials, J. Cult. Herit. 8 (2007) 223–234, doi:10.1016/j.culher.2007.06.001.
[18] S. Genkinger, A. Putnis, Crystallisation of sodium sulfate: supersaturation and metastable phases, Environ. Geol. 52 (2007) 295–303, doi:10.1007/s00254-006-0565-x.
[19] A.A.C. Bode, V. Vonk, F.J. Van Den Bruele, et al., Anticaking activity of ferrocyanide on sodium chloride explained by charge mismatch, Cryst. Growth Des. 12 (2012) 1919–1924, doi:10.1021/cg201661y.
[20] B. Lubelli, R.P.J. Van Hees, H.P. Huinink, C.J.W.P. Groot, Irreversible dilation of NaCl contaminated lime-cement mortar due to crystallization cycles, Cem. Concr. Res. 36 (2006) 678–687, doi:10.1016/j.cemconres.2005.10.008.
[21] T. Rivas, E. Alvarez, M.J. Mosquera, et al., Crystallization modifiers applied in granite desalination: the role of the stone pore structure, Constr. Build. Mater. 24 (2010) 766–776, doi:10.1016/j.conbuildmat.2009.10.031.
[22] J. Cassar, A. Marrocchi, M.L. Santarelli, M.L.S.M. Muscat, Controlling crystallization damage by the use of salt inhibitors on Malta's limestone, Mater. Construcción 58 (2008) 281, doi:10.3989/mc.2008.v58.i289-290.83.
[23] M. Franceschini, A. Broggi, M.P. Bracciale, et al., Effectiveness of phosphocitrate as salt crystallization inhibitor in porous materials: case study of the Roman Mosaic of Orpheus and the Beasts (Perugia, Italy), Int. J. Archit. Herit. 9 (2014) 195–200, doi:10.1080/15583058.2012.760121.
[24] S. Gupta, K. Terheiden, L. Pel, A. Sawdy, Influence of ferrocyanide inhibitors on the transport and crystallization processes of sodium chloride in porous building materials, Cryst. Growth Des. 12 (2012) 3888–3898, doi:10.1021/cg3002288.
[25] S. Gupta, L. Pel, M. Steiger, K. Kopinga, The effect of ferrocyanide ions on sodium chloride crystallization in salt mixtures, J. Cryst. Growth 410 (2015) 7–13, doi:10.1016/j.jcrysgro.2014.10.018.
[26] T. Rivas, J. Feijoo, I. de Rosario, J. Taboada, Use of ferrocyanides on granite desalination by immersion and poultice-based methods, Int. J. Archit. Herit. 11 (2017) 588–606, doi:10.1080/15583058.2016.1277282.
[27] B. Lubelli, T.G. Nijland, R.P.J. Van Hees, A. Hacquebord, Effect of mixed in crystallization inhibitor on resistance of lime-cement mortar against NaCl crystallization, Constr. Build. Mater. 24 (2010), doi:10.1016/j.conbuildmat.2010.06.010.
[28] S.J.C. Granneman, B. Lubelli, R.P.J. Van Hees, Characterization of lime mortar additivated with crystallization modifiers, Int. J. Archit. Herit. (2018) 1–10.
[29] S.J.C. Granneman, B. Lubelli, R.P.J. Van Hees, Effect of mixed in crystallization modifiers on the resistance of lime mortar against NaCl and Na2SO4 crystallization, Constr. Build. Mater. 194 (2019) 62–70, doi:10.1016/j.conbuildmat.2018.11.006.
[30] B. Lubelli, R.P.J. van Hees, C.J.W.P. Groot, Sodium chloride crystallization in a "salt transporting" restoration plaster, Cem. Concr. Res. 36 (2006) 1467–1474, doi:10.1016/j.cemconres.2006.03.027.
[31] B. Lubelli, Sodium Chloride Damage to Porous Building Materials, Delft University of Technology, 2006.
[32] Product information sheet - SanierGrundputz SG 68 (Baumiet). https://baumit.de/files/de/pdf_files/pdbl_saniergrundputz_sg_68.pdf. Accessed 12 Jul 2022
[33] Product information sheet - SanierPutz Fein 64F (Baumiet). https://baumit.de/files/de/pdf_files/pdbl_sanierputz_fein_sp_64_f.pdf. Accessed 12 Jul 2022
[34] C.J.W.P. Groot, Effects of Water on Mortar-Brick Bond, Delft University of Technology, 1993.
[35] van der Klugt L.J.A.R., Koek J.A.G. (1994) De kwaliteit van voegen in metselwerk. SBR
[36] B. Lubelli, R.P.J. Van Hees, H.J.P. Brocken, Experimental research on hygroscopic behaviour of porous specimens contaminated with salts, Constr. Build. Mater. 18 (2004) 339–348, doi:10.1016/j.conbuildmat.2004.02.007.
[37] M. Nasraoui, W. Nowik, B. Lubelli, A comparative study of hygroscopic moisture content, electrical conductivity and ion chromatography for salt assessment in plasters of historical buildings, Constr. Build. Mater. 23 (2009) 1731–1735, doi:10.1016/j.conbuildmat.2008.09.029.
[38] T. Diaz Gonçalves, J. Delgado Rodrigues, Evaluating the salt content of salt-contaminated samples on the basis of their hygroscopic behavior. Part I: fundamentals, scope and accuracy of the method, J. Cult. Herit. 7 (2006) 79–84, doi:10.1016/j.culher.2006.02.009.
[39] T.D. Gonçalves, J.D. Rodrigues, M.M. Abreu, Evaluating the salt content of salt-contaminated samples on the basis of their hygroscopic behaviour: part II: experiments with nine common soluble salts, J. Cult. Herit. 7 (2006) 193–200, doi:10.1016/j.culher.2006.03.002.

[40] M. Shirom, G. Stein, The absorption spectrum of the ferrocyanide ion in aqueous solution, Isr J. Chem. TA - TT 7 (1969) 405–412 - https://tudelft.on.worldcat.org/oclc/5185309555 , doi:10.1002/ijch.196900051 LK.
[41] C.N. Banwell, Fundamentals of Molecular Spectroscopy, Second Edi, McGraw - Hill Book Co, UK), 1972.
[42] F.P. Treadwell, W.T. Hall, Analytical Chemistry: Volume I, Qualitative Analysis, 9th editio, John Wiley and Sons Inc., New York, 1963.
[43] D.D. Kuhn, T.C. Young, Photolytic degradation of hexacyanoferrate (II) in aqueous media: the determination of the degradation kinetics, Chemosphere 60 (2005) 1222–1230, doi:10.1016/j.chemosphere.2005.02.011.
[44] C.E. Housecroft, A.G. Sharp, Inorganic Chemistry, Pearson Education, Harlow, 2005.
[45] B. Lubelli, J. Nijland, R.P.J. van Hees, A. Hacquebord, Effect of mixed in crystallization inhibitor on resistance of lime-cement motor against NaCI crystallization, Constr. Build. Mater. 24 (2010) 2466–2472.